Rare-earth-size effects on thermoluminescence and second-harmonic generation

2001 J. Phys.: Condens. Matter 13 2211

(http://iopscience.iop.org/0953-8984/13/10/315)

INSTITUTE OF PHYSICS PUBLISHING JOURNAL OF PHYSICS: CONDENSED MATTER

J. Phys.: Condens. Matter **13** (2001) 2211–2224 www.iop.org/Journals/cm PII: S0953-8984(01)17046-3

Rare-earth-size effects on thermoluminescence and second-harmonic generation

P D Townsend[1,7], A K Jazmati[2], T Karali[3], M Maghrabi[4], S G Raymond[5] and B Yang[6]

[1] EIT, Sussex University, Brighton BN1 9QH, UK
[2] Physics Department, AEC of Syria, Damascus, PO Box 6091, Syrian Arab Republic
[3] Ege University, Institute of Nuclear Sciences, 35100 Bornova, Izmir, Turkey
[4] CPES, Sussex University, Brighton BN1 9QH, UK
[5] Department of Physics, Eastern University, Chenkalady, Sri Lanka
[6] Department of Physics, Beijing Normal University, Beijing 100875, China

E-mail: p.d.townsend@sussex.ac.uk

Received 11 September 2000, in final form 11 January 2001

Abstract

The substitution of rare-earth ions into insulating host crystals introduces lattice strains and, for non-trivalent sites, a need for charge compensation. Such effects alter the site symmetry and this is reflected in properties such as the wavelength, linewidth, lifetime and relative intensity of the rare-earth transitions. Equally clear, but less well documented, is the influence on second-harmonic generation (even from cubic crystal lattices). For example, in bismuth germanate, second-harmonic generation efficiency varies by factors of more than 100 as a result of different rare-earth dopant ions. The ions are variously incorporated as substitutional ions, pairs, clusters, or even as precipitates of new phases, but the detailed modelling is often speculative. This article summarizes some recent studies which explore the role of rare-earth ions in thermoluminescence and second-harmonic generation. There are numerous differences in glow peak temperature, for nominally the same defect sites, which are thought to indicate charge trapping and recombination within coupled defect sites, or within a large complex. Size and cluster effects can be modified by heat treatments. This review considers the similarity and trends seen between numerous host lattices which are doped with rare-earth ions. For thermoluminescence there are trends in the variation in glow peak temperature with ion size, with movements of 20 to 50 K. Examples are seen in many hosts with extreme effects being suggested for zircon, with peak shifts of 200 K (probably from precipitate phases).

1. Introduction

Rare-earth activation of phosphors has long been seen as an effective process since coupling energy into the rare-earth-ion site, either by ionization, charge exchange or a resonance

[7] Author to whom any correspondence should be addressed.

energy process, results in light production. The efficiency is high, possibly because alternative pathways of excited-state relaxation, which dispel energy via phonon coupling to the surrounding lattice, are minimized and the value of the role of rare-earth (RE) ions in thermoluminescence (TL) dosimetry was rapidly recognized (Merz and Pershan 1967, Nambi *et al* 1974, Sunta 1984, McKeever 1985, McKeever *et al* 1995). The efficiency of conversion from the energy stored to optical output varies with the RE ion and good performance from many dosemeters is now achieved by activation with Dy or Tm. The Tm emission is particularly well matched to the blue/UV response of bialkali photomultiplier tubes, whereas the Dy lines are at longer wavelengths. Inevitably, any dopant ion that substitutes onto a lattice ion site introduces some mismatch with the host lattice in terms of ionic size and, except for trivalent sites, there will be a further mismatch in charge state. The RE ions are normally RE^{3+} and this is apparent from their emission spectra. There are a limited number of examples for RE^{2+} emission, for example from alkali halides and apatites (Aguirre de Carcer *et al* 1999, Kottaisamy *et al* 1994), but there are few unequivocal examples of substitution as either RE^{2+} or RE^{4+} ions, despite production of the divalent state being proposed in many TL models. Size and charge-state factors have lead to a diversity of conflicting models for the lattice accommodation of the RE ions. Early views were that if the ionic radius of the RE^{3+} ions is within a few per cent that of the host ion, then trivalent substitution is readily possible, and following irradiation, the RE becomes RE^{2+}, with positive charge being trapped elsewhere in the lattice. Subsequently, during the TL process it was assumed that the RE^{2+} reverts to RE^{3+} and emits light. This was a useful starting model but it disguises some major problems. Firstly, the 'ionic radius' differs with coordination number (and the method of assessing the value). Secondly, it is the lattice distortion caused by the volume of the ion which is relevant, and if the RE^{2+} ion is formed during dosimetry, then this ion must also be accommodated in the lattice. As a simple example, consider Dy replacing Ca in TL dosemeter systems such as CaF_2 or $CaSO_4$ where the Ca^{2+} 'radius' is $\sim$0.099 nm, and Dy^{3+} sizes are estimated to vary from 0.091 to 0.123 nm for coordination numbers from 6 to 12. The RE^{2+} radius is probably some 15% larger (as judged from data for other 3+ and 2+ RE ions). Thus size substitution of Dy^{3+} on a Ca^{2+} site is feasible, but the volume of the Dy^{2+} ion exceeds that of the Dy^{3+} ion on the Ca site by $\sim$50%. This would create a totally unacceptable lattice distortion.

For RE replacement into non-trivalent sites the key requirement is 'local' charge compensation. There are many alternative ways in which this can be achieved. The simplest is by addition of secondary impurity ions with a different valency from the host or RE ion. In the $CaSO_4$ example, local charge compensation can be achieved by substitution of secondary dopant ions (e.g. Na on an adjacent Ca site) which in turn modifies the cation structure. Equally there can be a metastable reorganization of host ions to a different charge state and numerous oxygen-related (or other anion-related) variants of intrinsic defect sites have been detected or postulated.

Focusing attention on single-ion sites was initially helpful (e.g. to predict optical transition energies of alkali halide F centres). However, as monitoring techniques have advanced, (e.g. with ESR, ENDOR, site-resolved exciton luminescence) it has become abundantly clear that the so-called 'point' defects introduce significant distortions in position and charge over a much larger volume of material. Recognition of the scale of these long-range interactions has surprisingly increased smoothly with time—figure 1—and it is now obvious that most insulators have no volume of their structure which can be considered to be perfect and free of defect interactions. For deliberately doped materials, such as RE-activated thermoluminescence dosemeters or laser materials, energy coupling between defect sites is guaranteed. The effects are apparent from high-resolution luminescence measurements that reveal long-range interactions extending over tens of neighbouring ion shells (i.e. encompassing

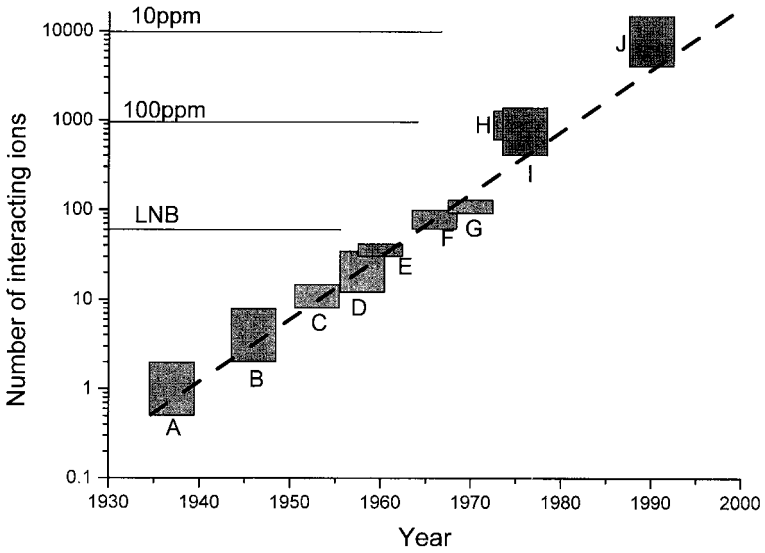

Figure 1. Changes in the perception of the interaction volume of 'point' defects with time. Assessments from A to J are variously based on optical absorption, photoluminescence, ESR, ENDOR, TL models, exciton luminescence and studies of colloids and nanoparticles. The volume of 'perfect' material is indicated for 10 and 100 ppm dopant levels and for congruent lithium niobate.

several dopants if they were randomly distributed). These considerations all support the concept that incorporation of RE ions may be energetically preferable via associations of several RE ions, lattice defects and structural distortions into relatively large defect complexes involving tens of ions. Indeed many such structures have been identified experimentally and justified by computer simulations. An early luminescence example revealed the formation of Cr pairs in ruby, where the strain caused by the much larger Cr ion on the Al site (the radii differ by $\sim$15%) results in strain energy minimization via impurity pairing and a new pair of emission lines at 700.4 and 703.3 nm (Schawlow *et al* 1959). The extreme consequence of clustering etc is where the energetics favour precipitation of new phases (e.g. to produce microcrystallites or nanoparticle inclusions). Familiar thermoluminescence examples, as reviewed in many places (Agullo Lopez *et al* 1988, Chen and McKeever 1997, McKeever *et al* 1995), include the LiF:Mg:Ti:O radiation dosemeters, where there is an immense literature showing that the added Mg ions form single, pair or trimer cluster variants of (Mg^{2+} + $Li_{vacancy}$) units that are directly linked to the Ti and O luminescence sites. Their formation occurs near the optimal TL doping level of $\sim$100 ppm of Mg. However, at even higher concentrations, the Mg destroys the normal LiF lattice to form precipitates of a new phase (termed the Suzuki phase (Suzuki 1961)). Precipitate examples are similarly well documented from the current interest in optical non-linearity of metal nanoparticles formed by ion beam implantation. The literature offers very many examples of TEM micrographs showing precipitation of excess metal into large nanoparticles with a wide range of sizes and, depending on the processing, growth of large units with a surrounding metal-denuded zone (e.g. Gonella 2000, Meldrum *et al* 2000). More complex processing, as with pulse laser anneals, can sometimes lead to a homogeneous dispersion of the metal dissolved into the host (Townsend and Olivares 1997). Of relevance to luminescence efficiency is that after ion implantation of rare-earth ions it is necessary to anneal the lattice damage. During this process the mismatch in ionic radii can induce RE clustering,

and a consequent quenching of their luminescence. Pulse laser annealing establishes a non-thermodynamic equilibrium where they are again effective, for example with enhancements in intensity of more than 100 times in some cases (Can *et al* 1995). Overall, these alternatives to thermodynamic equilibrium, as implied from furnace heating, underline the possibilities achievable for defects in non-thermodynamic equilibrium in the host insulator.

In principle, any changes in lattice parameter, site symmetry, secondary impurities as neighbours, growth of large-scale complex defects or phase transitions, should be reflected by spectral changes. Rare-earth dopants fit into this general pattern and have the advantage for analysis that the line spectra of shielded inner-shell transitions are both readily identifiable and respond to changes in local crystal field caused by variations in neighbouring site occupancy, pressure or phase. There are measurable changes detectable in linewidth, lifetime and wavelength. In photoluminescence the movements of the energy levels modify the absorption spectra and so one can present contour plots which emphasize both the similarities, and the differences, between rare-earth ions in a variety of related sites in the lattice. As reviewed in a recent text by Itoh and Stoneham (2001), changes in the relative size of the ions can introduce extremely major alterations. Itoh and Stoneham review the familiar Ivey–Mollwo energy shifts of absorption and luminescence with changing lattice parameter for alkali halides and also show the trend for self-trapped exciton luminescence rates which alter by some 10^6 for a 40% change in cation/anion ratio. Figure 2 shows one such example of site-selective spectroscopy for the infra-red emission from Er in $LiNbO_3$ (Herreros 1997). Several sites are apparent from the changes in excitation and emission spectra. Equally, the differences in lattice distortion caused by varying the size of impurity ions is reflected in many other optical properties such as the efficiency of second-harmonic generation (SHG) or electro-optic responses. Indeed, even cubic lattices doped with RE ions can show strong SHG signals since the strain caused by the RE-ion sites removes the cubic symmetry.

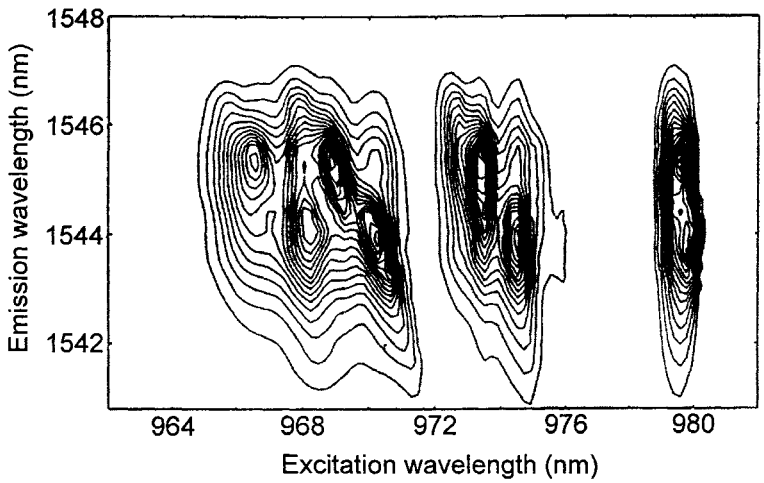

Figure 2. An example of site-selective spectroscopy for Er-doped $LiNbO_3$ in which site variations are revealed by differences in excitation and emission spectra (after Herreros 1997).

One of the standard responses of RE-impurity-controlled TL dosemeters is that the temperature of the glow peaks, and their spectra, are highly sensitive to secondary impurities and thermal processing. This is an important observation as it implies that the trapping sites are not independent of the RE luminescent sites. Additionally, the intensity response with dopant concentration is rarely linear, except over a limited and very low impurity range, (e.g. below say

10^{-2} mol% of Tm or Dy in $CaSO_4$) (Prokic 1978). At higher concentrations there is saturation of the TL performance (by ∼0.2 mol%) and by ∼4 mol% the signal is quenched. Even more spectacular dose dependence is seen from the Mn emission in calcite (Calderon *et al* 1996, Townsend *et al* 1999) where changes in impurity content of 100 can take the signals through an intensity peak range of more than 10^5. In that example, the various glow peaks display quite different responses to impurity concentrations. This further emphasizes that the Mn-controlled emission arises not only from different trapping sites but also from ones which are coupled to sites with different concentrations of Mn ions. Spatial images of samples taken during the TL confirm that the three main glow peaks are independently sensitive to the variations in Mn concentration (Hallensleben *et al* 1999a, b).

There have been attempts to separate the problems of charge compensation and ion-size effects in lattices where the RE ions substitute for trivalent host ions. Examples which explored this option include the TL from RE ions in LaF_3 (Yang *et al* 1998, Yang and Townsend 2000) or $Bi_4Ge_3O_{12}$ (Raymond *et al* 1994, Raymond and Townsend 2000). As shown for the LaF_3 data of figure 3, the peak movements demonstrate a smooth trend in glow peak temperature with ion size. The pattern indicates that small ions occupy sites with coordination numbers (CN) of 6, middle-size ions a CN of 8 and the La has a CN of 8. This implies that either the RE ions occupy different La sites, or the RE dopants distort the host lattice to modify the configuration, even for a small size mismatch.

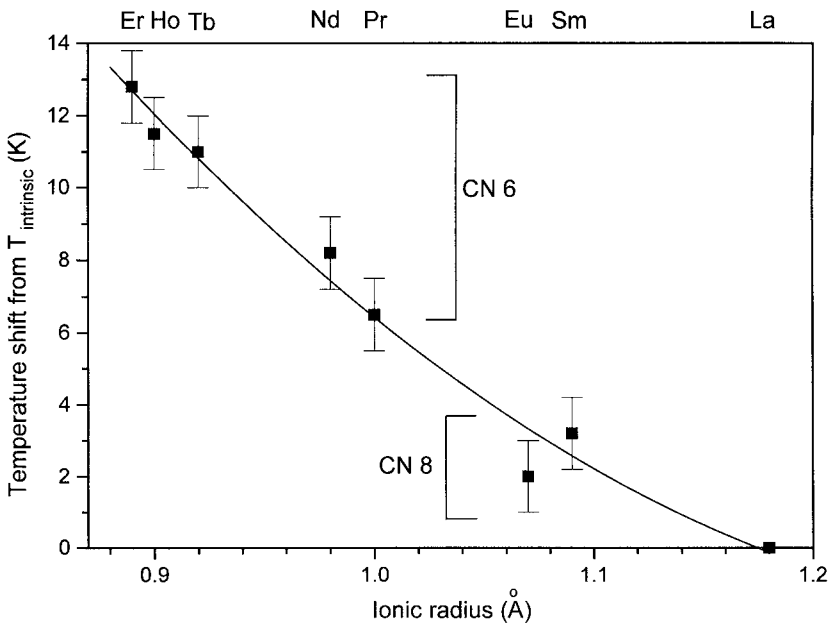

Figure 3. Changes in glow peak temperature relative to the intrinsic TL emission for RE-doped LaF_3. Note that different configuration numbers are required to describe the plot for small and large dopant ions (after Yang *et al* 1998).

2. A model for energy transfer to RE ions during TL

The preceding summary emphasizes that the inclusion of RE ions, to act as efficient luminescent sites, will distort the host lattice, and often require secondary impurities to offer local charge

compensation. Such structural rearrangements can favour the formation of complex sites in which there are strong interactions between the trapping and luminescent sites. The scale of the distorted lattices will variously extend from being limited to the RE ion and a few shells of neighbours, to entire zones of precipitates with differing structure and/or phase from the host lattice. Such assemblies of non-standard structures may be sufficiently large that they provide all the necessary conditions for energy storage, in the form of charge separation, which is the pre-requisite for thermoluminescence dosimetry. One can therefore offer a model of the reasons for high TL efficiency for RE-doped material in which the original radiation of the dosemeter generates electrons and holes which can move within the lattice structure. These are preferentially trapped within the extended and distorted lattice regions which encompass the RE ion, and where needed, the charge compensation. The subsequent TL readout of the dosimetry information results in charge release localized within the complex. This is followed by electron–hole recombination that closely resembles the generation of excited-state excitons and, as for excitons, the excited-state lifetimes are sufficiently long that there can be local lattice relaxation and energy transfer from the electron–hole pair to the RE^{3+} ion. The emission will be characteristic of the RE ion, which has remained trivalent. The TL is thus achieved without the problems of accommodation of oversize RE^{2+} ions. A crucial prediction of this model is that the RE is within the complex that contains the trapping site, and therefore the distortions created by RE ions of different size will strongly influence the stability of the trap. The variations may show in changes either in vibrational frequency or in trap depth. In each case the result will be glow peaks which differ in temperature in a systematic way depending on the ionic sizes of the RE dopants. High TL efficiency is inevitable as the energy was selectively stored in close proximity to the RE ion.

Experimental features which could support this model are:

(a) TL peak temperatures changing as a function of ionic size;
(b) first-order kinetics for this highly directed recombination that leads directly to energy transfer and RE emission;
(c) wavelength shifts resulting from the crystal-field interactions of the RE ion in a distorted region of the lattice.

Further, there are likely to be:

(d) differences in the relative intensities of the emission lines between radioluminescence (RL) or cathodoluminescence (CL) and TL—the RL and CL will activate high-level states of the RE ions and those within the conduction band, but TL from energy transfer (such as excited-exciton relaxation) will only be able to stimulate lower-state transitions.

There will be

(e) sensitivity to concentration as pairing or clustering will reduce the efficiency per RE ion, as well as introducing wavelength changes from the new local environment—some effects will be thermally activated whilst others will arise via energy transfer; particularly clear examples are known for Er ions that have long-lived states (a feature exploited in upconversion).

Finally,

(f) sensitivity to heat treatments can exist. Depending on the temperature range, and rate of sample cooling, normal furnace treatments can influence either growth, or dissolution of clusters, but more exotic thermal processing, such as pulsed laser annealing, may introduce spectacular (non-thermodynamic) changes. Laser treatments has been shown to induce metastable phases, which in the case of glass hosts may even be crystalline (Townsend *et al* 1996).

3. Examples of spectral change and variations in glow peak temperature

Conventional TL radiation dosimetry systems are optimized to generate high detection sensitivity and reproducibility, and indeed perform excellently, but for consideration of the points indicated above a different experimental emphasis is required. For example it is necessary to use low heating rates in order to avoid the normally significant temperature gradients which exist between the heater stage and the sample (Betts *et al* 1993, Betts and Townsend 1993, Townsend *et al* 1997). Detailed spectrally resolved data are also crucial, and where possible, the spectra should be accumulated via a high-resolution wavelength-multiplexed spectrometer. Unfortunately very few spectral systems have been built for TL analysis, and even fewer with wavelength multiplexing. As is apparent from the items cited here, such analysis is highly informative and opens many new research perspectives. The numerous citations to work from Sussex are merely the consequence of a high-sensitivity TL spectral system (Luff and Townsend 1993) rather than any intentional reporting prejudice. Data at low temperature can be highly informative, as they can respond to the presence of intrinsic point defects, many of which (such as the interstitial and hole centres) anneal out below say 150 K (Agullo Lopez *et al* 1988, Hayes and Stoneham 1985, Itoh and Stoneham 2001). In general, vacancy defects and larger defect clusters are stable to higher temperatures than the simpler defects. Low-temperature studies have been made less frequently than those above room temperature both for experimental reasons and because they are not of relevance to dosimetry. Information on the relative number of excited states is offered by comparisons between TL and RL. Recent work at Sussex has examined the influence of RE ions in both conventional dosemeter materials (CaF_2, $CaSO_4$, MgB_4O_7), and other materials such as LaF_3, $Bi_4Ge_3O_{12}$, SrF_2, BaF_2 and zircon. Nearly all of the samples offer very strong evidence for RE defect complexes with the behaviours predicted above. A very rapid summary of key observations from the Sussex data which exploit the spectral information is now tabulated. Additionally the wider literature includes numerous examples on the influence of secondary impurities on glow peak temperature (T_{max}).

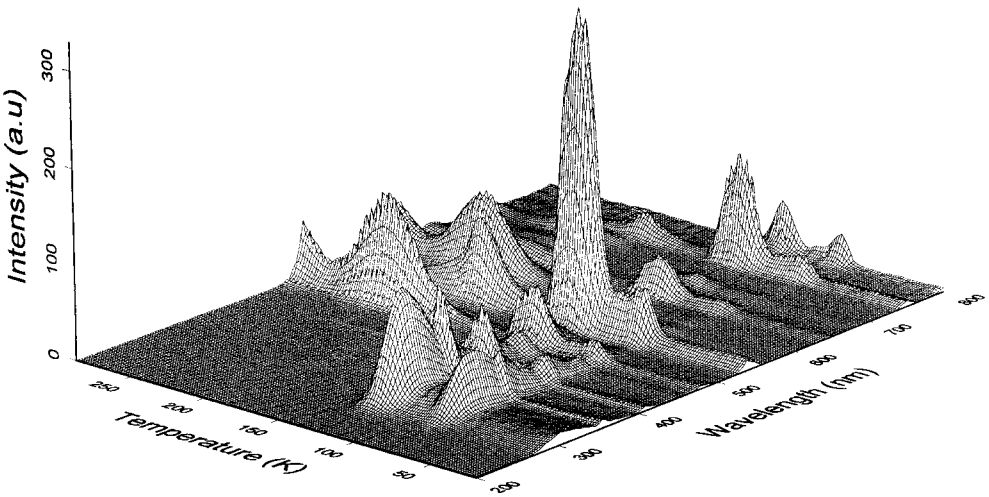

Figure 4. An isometric view of the TL emission spectra from LaF_3 containing both Ho and Pr dopants. Note that the spectra define RE-specific glow peak temperatures.

3.1. LaF_3:RE

As shown by figure 3 (Yang *et al* 1998) there are systematic differences between intrinsic TL peak temperatures and RE signals as a function of ion size, with maximum T_{max} shifts of ∼20 K across the range of lanthanide dopants. Coordination numbers of 6 and 8 for small and middle-size ions are required to reveal this smooth trend. Similar data for higher-temperature peaks (Yang and Townsend 2000) show either first-order kinetics with high-frequency factors, or mixed order kinetics with lower-frequency terms. T_{max}-values change with both concentration and heat treatments and in these cases the component peaks are found by analysis to have values of E (energy) and S (frequency factor) which are greatly reduced. Co-doped sample data have T_{max}-values consistent with clusters from at least three RE ions per complex. Figure 4 demonstrates the spectrally resolved TL with an isometric plot of low-temperature TL data for a sample intentionally containing Ho, but from the spectra, also with traces of Pr. The plot of figure 4 emphasizes how the emission for the different RE ions occurs at distinctly different temperatures in which intrinsic broad-band emission occurs in the UV. Ho lines are seen near 135 K and Pr signals nearer 200 K.

3.2. $Bi_4Ge_3O_{12}$:RE

Above room temperature, T_{max} shifts by ∼10 K and scales with the vibrational frequency changes caused by the mass range of the RE ions, suggesting that a substitutional RE ion is adjacent to a vacancy (Raymond *et al* 1994). At low temperature (Raymond and Townsend 2000), the peaks move with the difference in ion size relative to the Bi^{3+} size, as for the LaF_3 data, but in this case the Bi-ion size is not at the extreme limit of the size range (figure 5). Movements are up to 20 K for the three main low-temperature peaks with the lowest temperatures seen for the intrinsic trivalent-ion case (i.e. Bi^{3+}).

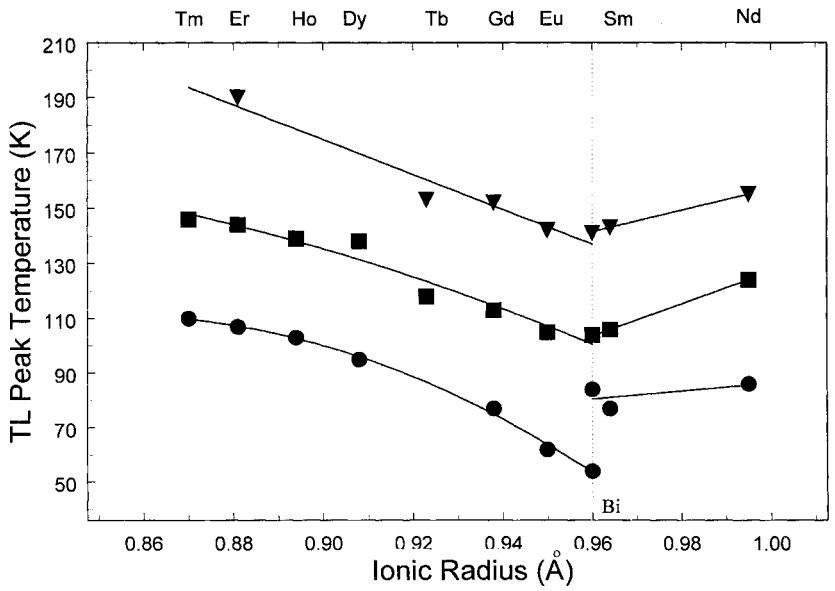

Figure 5. Movement of glow peaks as a function of RE-ion size for RE-doped $Bi_4Ge_3O_{12}$. The intrinsic material has the peaks at lowest temperatures (Raymond and Townsend 2000).

3.3. $CaSO_4$:Dy/Tm

In either separately, or co-doped material, Dy and Tm dosimetry signals (nominally near 200 °C) differ by ∼8 K (Karali *et al* 1998, 1999). Additions of Ag or Ce to the lattice introduce numerous TL changes and raise the dosimetry peak to ∼400 °C (Maghrabi *et al* 2000). Concentration-dependent effects for RL data at high concentration suggest either three or four RE ions per complex and pulsed laser heating introduces a major and discontinuous wavelength shift in the emission at temperatures of ∼210 and 275 °C. Such a pattern is characteristic of phase change seen in other materials and in this case it is thought to be a phase effect of the environment surrounding the TL site.

3.4. MgB_4O_7:Dy/Tm

In co-doped material, Dy and Tm dosimetry signals differ by ∼30 K (Karali *et al* 1999).

3.5. CaF_2:Nd

The TL spectra differ between glow peaks above room temperature and, although they are consistently linked to transitions from Nd, the relative intensities of the signals from different starting manifolds are strongly concentration dependent. For some mid-range concentrations it was possible to alter the emission between two patterns by annealing followed by either fast or slow cooling. The interpretation offered was that the heat treatments allowed impurity cluster formation during slow cooling, whereas rapid cooling achieved a non-thermodynamic equilibrium by freezing in the dispersed ions which existed as isolated ions dissolved in the lattice at high temperature (Holgate *et al* 1994). In other luminescence studies the structure seen by high resolution of the emission lines was attributed variously to single, pairs of and clusters of RE ions per site (Bausa *et al* 1991). Whilst no detailed models have been proposed, all of the discussions of RE defect sites appear to require interactions involving many lattice sites, including charge compensators and/or intrinsic lattice sites.

3.6. BaF_2:RE; CaF_2:RE; SrF_2:RE

Visually there are some broad similarities in the glow peak temperatures between the shapes of the various RE glow curves for all of this set of crystals, and even greater consistency emerges in terms of component peak temperatures following kinetic analyses. By contrast with the example of LaF_3, there are no major peak shifts of T_{max} with different RE ions, although some minor changes are observed from ion-size effects, with others related to concentration. There are significant differences in the relative intensities of the component peaks with different RE dopants (Maghrabi 2001).

3.7. Zircon:RE

Synthetic samples show apparently totally disparate glow curves with RE doping; nevertheless, on closer analysis of the component peaks there appear to be sets of signals which can be linked via a RE-size-dependent trend. The peak positions fit remarkably well to a linear plot of T_{max} with RE size. Data are presented in figure 6 for the two lowest sets of strong glow peaks. The important fact to note is that the range of the movement of T_{max} is very large, being some 200 K (Karali *et al* 2000).

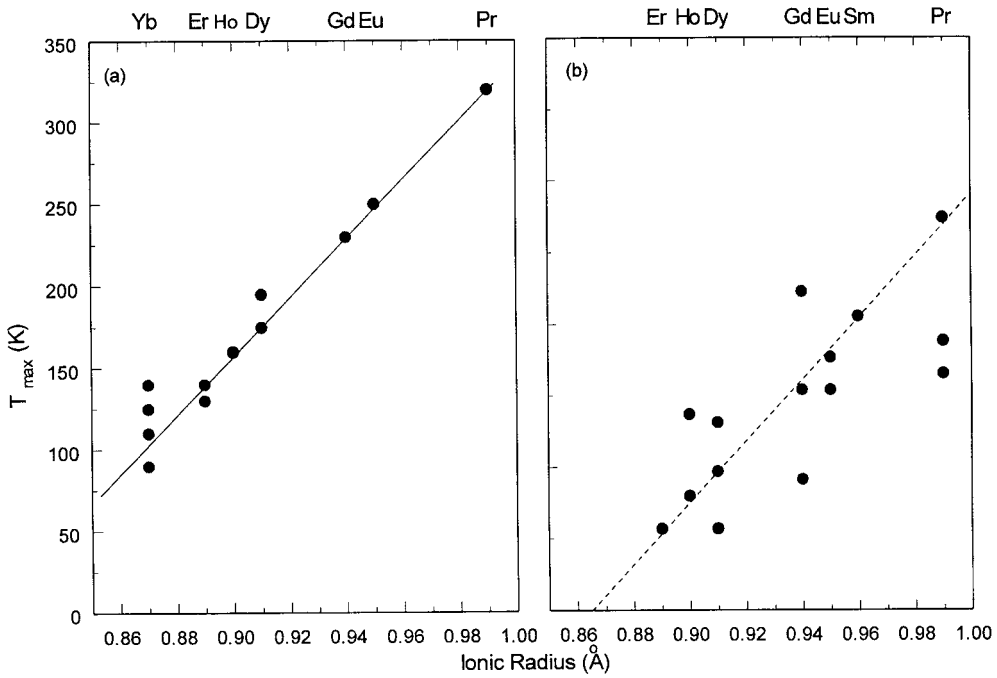

Figure 6. RE-size effects on TL peaks from zircon. Note that the trends appear to span almost 200 K (Karali *et al* 2000).

4. Linewidths and second-harmonic generation in $Bi_4Ge_3O_{12}$:RE

As indicated in the introduction, distortions caused by substitution of a rare-earth ion (even onto a trivalent lattice site) will have a measurable influence on both the linewidth and the production of second-harmonic generation (SHG). Such effects have been noted by several groups for RE ions in $LiNbO_3$, and other hosts, but for the present purpose it is convenient to compare the changes with the preceding thermoluminescence data. In parallel with the TL studies of $Bi_4Ge_3O_{12}$:RE the material was formed into optical waveguides by ion beam implantation, and the photoluminescence (Jazmati and Townsend 2000) and efficiency for SHG (Jazmati *et al* 2000) were monitored. The SHG signals give a particularly clean response to the lattice distortion of the cubic host material. Figures 7 and 8 show how there is both line broadening and increased SHG efficiency in the waveguide material, which increases with annealing temperature after implantation. The SHG pattern is emphasized further by increasing the pump power. In both types of measurement the minimum response is for the ions which are closest in size to the Bi^{3+} ion for which they substitute, and the data resemble those for the TL ion-size response shown in figure 5. A broadly similar pattern has been discussed by Ellen *et al* (1997) for electron–phonon coupling in this host.

5. Discussion

An overview of the data summarized above is that there are broadly three classes of behaviour resulting from the inclusion of the RE luminescence sites in the insulating crystals considered here. These are epitomized by the alkaline-earth halides, the trivalent-site structures and zircon.

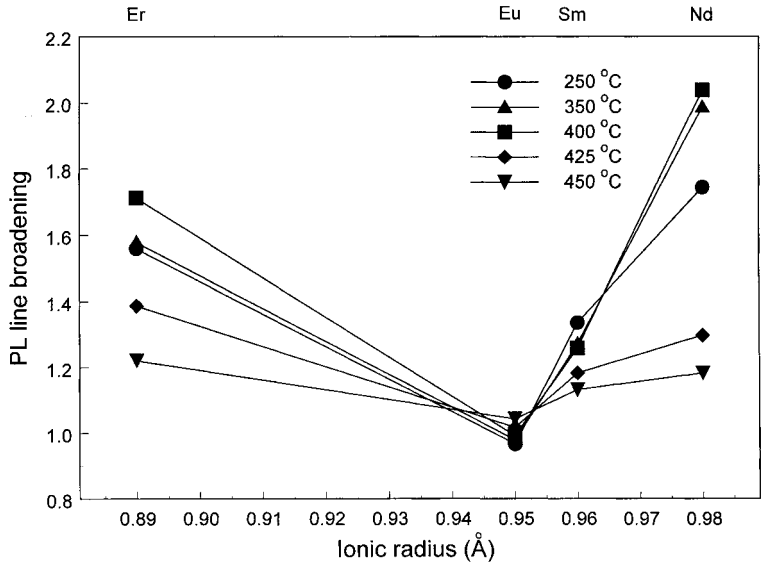

Figure 7. Photoluminescence line broadening from $Bi_4Ge_3O_{12}$ ion-implanted waveguides, relative to signals from bulk material. The distortions, generated by He-ion implantation to form the guides, are reduced on annealing (Jazmati and Townsend 2000).

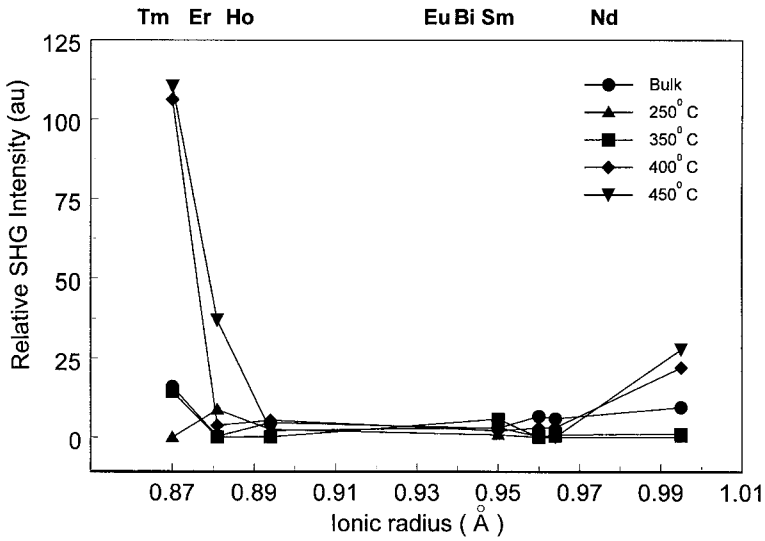

Figure 8. Surface second-harmonic generation from RE-doped $Bi_4Ge_3O_{12}$, as for figure 7 (Jazmati *et al* 2000).

For the alkaline-earth fluorides there is certainly strong evidence from the TL, as well as from the many earlier colour centre studies (Hayes 1974, Hayes and Stoneham 1985, Agullo Lopez *et al* 1988), that incorporation of RE ions is by substitution onto an alkaline-earth site, but as a result of size considerations, as well as the charge mismatch, there is a considerable influence on the local lattice structure. This can involve perhaps ten or more lattice sites, and also include development of RE ions existing in pairs, or larger groups, that are in

immediate proximity. Concentration effects and/or heat treatments modify these structures and have a clear influence on the emission spectra. However, the charge-trapping sites and luminescence complexes are effectively independent; thus there are minimal changes in the glow peak temperature with variations in RE-ion size.

In the cases of LaF_3 and $Bi_4Ge_3O_{12}$ it is strongly evident that the presence of trivalent RE ions substituted onto trivalent sites has a major effect on the apparent position of T_{max} for each of the main glow peaks. It is therefore a reasonable assumption that the same basic defect structures exist in each case but the RE ions interact so strongly with the charge traps that their bonding energies are shifted. The variations are significant, being from say 128 K for intrinsic signals, rising to 142 K for the smallest dopant ions in LaF_3. These main signals have first-order characteristics with a high pre-exponential factors ($\sim 10^{12}$ s^{-1}). This is also consistent with direct charge recombination within a large defect complex, but the fact that only trivalent emission lines are seen supports the model in which the electron–hole recombination energy resonantly transfers into the RE site. Note that, particularly for Eu dopants, the Eu^{2+} would provide an unequivocally different signature from that of the Eu^{3+} ions (Townsend and Rowlands 1999, Townsend 2001).

The sets of glow peak signals which are particularly sensitive to concentration and heat treatments generally have much lower frequency factors ($\sim 10^7$ s^{-1}) as might be expected for complexes which involve interactions from adjacent RE ions within the same complex. Such defect packages could then show responses with both very low E- and S-values.

The third class of response is displayed by the zircon samples. These appear to show totally different glow curves for the variously doped samples. Nevertheless, closer inspection of the data reveals component peaks with a pattern in which the signals are temperature shifted by up to 200 K with ion size—figure 6. Such a situation indicates a very strong interaction between the RE luminescence site and the region where charge is stored after irradiation. The immediate conclusion is that the TL results from within a large complex. However, it would appear to be inconceivable if this is merely the result of distortion of a simple defect. A far more plausible argument is that the RE ions precipitate out to form microphase complexes within the zircon—in which case the apparent lattice parameters of these units can differ significantly, with a consequent shift in peak temperature of the glow curves. There is therefore an immediate parallel with early examination of the annealing and TL response from the alkali halides in which the H-, V_K- and F′-related TL signals and annealing temperatures were previously related directly to the lattice parameter. The data are reproduced in figure 9 and show movements of some 200 K across the range of alkali halides in which the lattice parameters vary by a factor of two (Townsend *et al* 1967).

6. Conclusions

The emerging patterns from these data are that defect sites are complex, and the relatively minor differences in size distortion introduced by various rare-earth dopants lead to measurable optical changes. The preceding examples emphasize such effects from changes in TL peak temperature, SHG efficiency and photoluminescence line broadening. It is also clear that incorporation of the RE ions into different lattices is dramatically different as regards the scale of the changes, particularly if there is a consequent clustering or precipitation of the dopant ions from the host lattice. The trends are probably typical of many host systems. For future studies it will be desirable to use wavelength-multiplexed TL spectra with wavelength resolution sufficient to separate site-selective behaviour. This is an experimental challenge which has yet to be met.

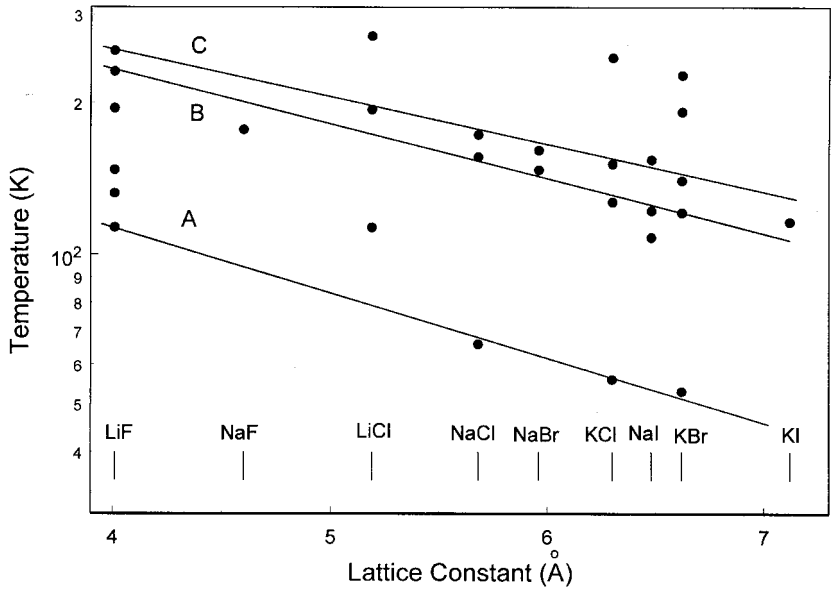

Figure 9. Data which relate the lattice parameter, TL and annealing stages of H, V_K and F′ centres in alkali halides, as indicated by lines A, B and C (after Townsend *et al* 1967).

References

Aguirre de Carcer I, Jaque F and Townsend P D 1999 Thermoluminescence of KI:Eu^{2+} stimulated by ultraviolet irradiation at different temperatures *Radiat. Protect. Dosim.* **84** 151–4

Agullo Lopez F, Catlow C R C and Townsend P D 1988 *Point Defects in Materials* (London: Academic)

Bausa L E, Legros R and Munoz-Yague A 1991 Effect of Nd^{3+} concentration on the emission spectra of CaF_2:Nd layers grown by molecular beam epitaxy *J. Appl. Phys.* **70** 4485–9

Betts D S, Couturier L, Khayrat A H, Luff B J and Townsend P D 1993 Temperature distribution in thermoluminescence experiments: I. Experimental results *J. Phys. D: Appl. Phys.* **26** 843–8

Betts D S and Townsend P D 1993 Temperature distribution in thermoluminescence experiments: II. Some calculational models *J. Phys. D: Appl. Phys.* **26** 849–57

Calderon T, Townsend P D, Beneitez P, Garcia-Guinea J, Millan A, Rendell H M, Tookey A, Urbina M and Wood R A 1996 Crystal field effects on the thermoluminescence of manganese in carbonate lattices *Radiat. Meas.* **26** 719–31

Can N, Townsend P D, Hole D E, Snelling H V, Ballesteros J M and Afonso C N 1995 Enhancement of luminescence by pulse laser annealing of ion implanted europium in sapphire, silica *J. Appl. Phys.* **78** 6737–44

Chen R and McKeever S W S 1997 *The Story of Thermoluminescence and Related Phenomena* (Singapore: World Scientific)

Ellen A, Andres H, ter Heerdt M L H, Wegh R T, Meijerink A and Blasse G 1997 Spectral line broadening study of the tri-valent lanthanide series: the variation of the electron–phonon coupling strength through the series *Phys. Rev.* B **55** 180–6

Gonella F 2000 Nanoparticle formation in silicate glasses by ion beam based methods *Nucl. Instrum. Methods* B **166+167** 831–9

Hallensleben S, Karali T, Rowlands A R and Townsend P D 1999a Correlations between thermoluminescence spectra and photon imaging of non-uniform samples *Radiat. Eff.* **149** 159–65

Hallensleben S, Rowlands A P, Karali T and Townsend P D 1999b Photon imaging of thermoluminescence *Radiat. Protect. Dosim.* **84** 115–8

Hayes W (ed) 1974 *Crystals with the Fluorite Structure* (Oxford: Oxford University Press)

Hayes W and Stoneham A M 1985 *Defects and Defect Processes in Nonmetallic Solids* (New York: Wiley)

Herreros B 1997 *Doctoral Thesis* Universidad Autonoma de Madrid

Holgate S A, Sloane T H, Townsend P D, White D R and Chadwick A V 1994 Thermoluminescence of calcium

fluoride doped with neodymium *J. Phys.: Condens. Matter* **6** 9255–66
Itoh N and Stoneham A M 2001 *Materials Modification by Electronic Excitation* (Cambridge: Cambridge University Press)
Jazmati A K and Townsend P D 2000 Photoluminescence from RE doped BGO waveguides *Nucl. Instrum. Methods* B **166+167** 597–601
Jazmati A K, Vazquez G and Townsend P D 2000 Second harmonic generation from RE doped BGO waveguides *Nucl. Instrum. Methods* B **166+167** 592–6
Karali T, Can N, Townsend P D, Rowlands A P and Hanchar J 2000 Radioluminescence and thermoluminescence of rare earth element and phosphorus-doped zircon *Am. Mineral.* **85** 668–81
Karali T, Rowlands A P, Townsend P D, Prokic M and Olivares J 1998 Spectral comparison of Dy, Tm and Dy/Tm in $CaSO_4$ thermoluminescent dosimeters *J. Phys. D: Appl. Phys.* **31** 754–65
Karali T, Townsend P D, Prokic M and Rowlands A P 1999 Comparison of the thermally stimulated luminescence spectra of codoped dosimetric materials *Radiat. Protect. Dosim.* **84** 281–4
Kottaisamy M, Jagannathan R, Jeyagopal P, Rao R P and Narayanan R L 1994 Eu^{2+} luminescence in $M_5(PO_4)_3X$ apatites where M is Ca^{2+}, Sr^{2+} and Ba^{2+}, and X is F^-, Cl^-, Br^- and OH^- *J. Phys. D: Appl. Phys.* **27** 2210–5
Luff B J and Townsend P D 1993 High sensitivity thermoluminescence spectrometer *Meas. Sci. Technol.* **4** 65–71
Maghrabi M 2001 to be published
Maghrabi M, Karali T, Townsend P D and Lakshmanan A R 2000 Luminescence spectra of $CaSO_4$ with Ce, Dy, Mn and Ag codopants *J. Phys. D: Appl. Phys.* **33** 477–84
McKeever S W S 1985 *Thermoluminescence of Solids* (Cambridge: Cambridge University Press)
McKeever S W S, Moscovitch M and Townsend P D 1995 *Thermoluminescence Dosimetry Materials: Properties and Uses* (Ashford, Kent: Nuclear Technology Publishing)
Meldrum A, Boatner L A, White C W and Ewing R C 2000 Ion irradiation effects in non-metals: formation of nanocrystals and novel microstructures *Mater. Res. Innovat.* **3** 190–204
Merz J and Pershan P 1967 Charge conversion of irradiated rare earth ions in calcium fluorides *Phys. Rev.* **162** 217–35
Nambi K S V, Bapat V N and Ganguly A K 1974 Thermoluminescence of $CaSO_4$ doped with rare earths *J. Phys. C: Solid State Phys.* **7** 4403–15
Prokic M 1978 Improvement of the thermoluminescence properties of the non-commercial dosimetry phosphors $CaSO_4$:Dy and $CaSO_4$:Tm *Nucl. Instrum. Methods* **151** 603–8
Raymond S G, Luff B J, Townsend P D, Feng Xiqi and Hu Guanqing 1994 Thermoluminescence spectra of doped $Bi_4Ge_3O_{12}$ *Radiat. Meas.* **23** 195–202
Raymond S G and Townsend P D 2000 The influence of rare earth ions on the low temperature thermoluminescence of $Bi_4Ge_3O_{12}$ *J. Phys.: Condens. Matter* **12** 2103–22
Schawlow A L, Wood D L and Clogston AM 1959 Electronic spectra of exchange coupled ion pairs in crystals *Phys. Rev. Lett.* **3** 271–3
Sunta C M 1984 A review of thermoluminescence of calcium fluoride, calcium sulphate and calcium carbonate *Radiat. Protect. Dosim.* **8** 25–44
Suzuki K 1961 X-ray studies on precipitation of metastable centres in mixed crystals NaCl–$CdCl_2$ *J. Phys. Soc. Japan* **16** 67–78
Townsend P D 2001 How big is a point defect? *Radiat. Eff.* at press
Townsend P D, Clark C D and Levy P W 1967 Thermoluminescence in lithium fluoride *Phys. Rev.* **155** 908–17
Townsend P D, Karali T, Rowlands A P, Smith V A and Vazquez G 1999 Recent examples of cathodoluminescence as a probe of surface structure and composition *Mineral. Mag.* **63** 211–26
Townsend P D and Olivares J 1997 Laser processing of insulator surfaces *Appl. Surf. Sci.* **110** 275–82
Townsend P D and Rowlands A P 1999 Extended defect models for thermoluminescence *Radiat. Protect. Dosim.* **84** 7–12
Townsend P D, Rowlands A P and Corradi G 1997 Thermoluminescence during a phase transition *Radiat. Meas.* **27** 31–6
Townsend P D, Wood R A, Brocklesby W, Brown R S and Townsend J E 1996 Thermoluminescence evidence for laser induced crystallisation of Tm doped germanosilicate fibres *Radiat. Protect. Dosim.* **65** 363–8
Yang B and Townsend P D 2000 Patterns of glow peak movement in rare earth doped LaF_3 *J. Appl. Phys.* **88** 6395–402
Yang B, Townsend P D and Rowlands A P 1998 Thermoluminescence of LaF_3 *Phys. Rev.* B **57** 178–88